Diffusion of Polystyrene Probes in Semidilute Poly(vinyl methyl ether) Solutions Confined in a Porous Glass Bead

Iwao Teraoka,*,† Ziming Zhou,‡ Kenneth H. Langley,‡ and Frank E. Karasz§

Department of Chemistry, Polytechnic University, 333 Jay Street, Brooklyn, New York 11201, and Department of Physics and Astronomy and Department of Polymer Science and Engineering, University of Massachusetts, Amherst, Massachusetts 01003

Received January 6, 1995; Revised Manuscript Received October 18, 1995⊗

ABSTRACT: Tracer diffusion processes were studied using dynamic light scattering for polystyrene (PS) probe molecules in semidilute solutions of a poyl(vinyl methyl ether) (PVME) matrix confined in a porous glass bead. The porous silica medium was equilibrated with the ternary solution containing PS, PVME, and the common solvent 2-fluorotoluene. Three-way refractive index-matching between the PVME, the solvent, and the silica facilitated the extraction of diffusion data from the light-scattering autocorrelation functions. Unlike the less miscible system of PS, poly(tetrahydrofuran), and 2-fluorotoluene reported earlier, the tracer diffusion coefficient in the porous medium decreased monotonically as the concentration of PVME increased in the exterior solution. The decrease in the tracer diffusion coefficient at high matrix concentrations was similar in form between the interior of the porous medium and the exterior solution for three different molecular weight fractions of PS. The results of the center of mass tracer diffusion in the pore channels were analyzed in terms of reptation and constraint release mechanisms. In the molecular weight range studied, the data support the latter mechanism.

Introduction

Entangled linear chain molecules exhibit a variety of dynamic modes over different length and time scales.[1,2] This diversity arises from topological interaction between neighboring chains. We can expect a further drastic change in the dynamic modes when the polymer chains are geometrically confined, for example, by porous materials with cavity sizes comparable to the chain dimensions.

The last decade has seen an advancement of experimental techniques[3−6] to study the dynamics of molecules in the interior of a controlled pore glass, a typical porous medium. Among others, dynamic light scattering (DLS) has taken advantage of refractive index-matching to enhance sensitivity and has been used intensively.[5−7] In brief, a focused laser beam is incident on a porous glass bead immersed in a solvent isorefractive with silica, the solid phase of the porous glass. The motion of any solvated polymer with a refractive index different from that of the solvent can then be traced by light scattering from within the porous glass. In a series of experiments, the diffusion coefficient of polymer molecules in the interior of the porous medium was first measured as a function of the molecular weight and of the pore size.[6,8] Secondly, the diffusion coefficient was measured[9] as the concentration c_E of the polymer in the exterior solution, in equilibrium with the porous medium, was increased beyond the overlap concentration c^*. In this case a large increase in the mutual diffusion coefficient was observed for polymers in the pore, ascribed to a sharp increase in the interior polymer concentration.[9] At low exterior concentrations, $c_E \ll c^*$, most polymer molecules are partitioned into the exterior solution, but a weak-to-strong penetration transition takes place in the partitioning of the polymer as c_E exceeds c^*.[9,10]

Recently, we also reported DLS measurements for a ternary polymer solution in a porous glass bead.[11] The diffusion of the polystyrene (PS) probe was monitored as the matrix poly(tetrahydrofuran) (PTHF) increased in concentration c_{mE} exterior to and therefore also within the pore channels. This measurement was facilitated by index-matching between PTHF, silica, and the solvent 2-fluorotoluene (2FT). In contrast to the increase in the mutual diffusion coefficient, we observed a decrease in the tracer diffusion coefficient D_p in the pore as well as in the tracer diffusion coefficient D_f in the exterior solution as c_{mE} increased in the range below the overlap concentration c_m^* of the pure matrix polymer. The decrease in D_p was larger than the decrease in D_f when compared at the same exterior concentration c_{mE}. Since the matrix concentration in the pore was estimated to be about $^1/_{10}$th of that in the exterior for the PTHF−porous glass bead system studied, the magnitude of the first-order concentration coefficient in D_p was thought to be at least 1 order of magnitude larger than that in D_f. We ascribed the large negative coefficient for D_p to an enhanced chain−chain interaction in the narrow, quasi one-dimensional pore channels that increases the effective friction retarding translation at finite polymer concentrations. The measurements of D_p and D_f were, however, limited to relatively low accessible matrix concentrations ($c_{mE}/c_m^* \lesssim 3.5$) because of the immiscibility of PS and PTHF, with phase separation occurring at higher c_{mE}. At the highest matrix concentrations measured, the decrease in D_p slowed down for the ternary solution system containing a low PS molecular weight fraction. This phenomenon was not observed in the exterior solution in the same concentration range of the exterior matrix PTHF. The difference between D_p and D_f at high concentrations may also indicate the enhanced interaction between repulsive polymer chains in the pore channels. It is interesting to note that a slowing-down in a decrease of D_f followed by an upturn has been reported for another incompatible ternary solution (in free solution)

† Polytechnic University.
‡ Department of Physics and Astronomy, University of Massachusetts.
§ Department of Polymer Science and Engineering, University of Massachusetts.
⊗ Abstract published in *Advance ACS Abstracts,* December 1, 1995.

0024-9297/96/2229-0037$12.00/0

consisting of polystyrene, polyisobutylene (PIB), and a common solvent.[12,13] Currently, this upturn is interpreted[13,14] in terms of a transition from the center of mass diffusion of the probe chain to a motion simulating the cooperative diffusion of entangled matrix chains as the solution system approaches phase separation.

In contrast to the situation in this relatively immiscible polymer−polymer system, a ternary solution in which polymer components are highly miscible did not exhibit a slowing-down or an upturn in D_f. Lodge and co-workers[15−18] studied the tracer diffusion coefficient D_f of PS in a poly(vinyl methyl ether) (PVME) matrix in the common solvent 2FT over a wide range of the matrix concentration c_{mE}. They were able to increase c_{mE} without being compromised by phase separation. As c_{mE} increased, D_f decreased monotonically. When the matrix chains were entangled, at the highest concentrations studied, they observed a power dependence $D_f \propto (c_{mE})^{\beta_f}$ with $\beta_f \cong -3.3$.[17,18] The large magnitude of the exponent β_f suggested an effective Θ-solvent condition[1] for PS molecules at high PVME concentrations. When there was a large difference in molecular weight between the probe polymer and the matrix polymer, an additional power dependence $D_f \propto M^{\alpha_f}$ was found to hold at high matrix concentrations, where M is the molecular weight of the probe PS. Lodge et al. observed[17,18] that the exponent was $\alpha_f \cong -1$ when the probe chain was the longer and $\alpha_f \cong -2$ when the matrix chain was the longer. These two exponents agreed with theoretical predictions of probe chain diffusion by constraint release and reptation mechanisms,[1] respectively.

More recently, Nyström and Roots[19] reanalyzed existing data for tracer diffusion coefficients in ternary solution systems that include (1) a high molecular weight PIB probe in a chloroform solution of low molecular weight PIB,[20,21] (2) PS in a 2FT solution of PVME,[17,18] (3) PS in a benzene solution of poly(methyl methacrylate) (PMMA),[22] and (4) PMMA in a thiophenol solution of PS.[23] They plotted D_f/D_{f0}, where D_{f0} is the tracer diffusion coefficient in the dilute solution limit of the matrix polymer, as a function of a reduced concentration proportional to c_{mE}/c_m^*. They showed that, except for the first ternary system, D_f/D_{f0} decreases at high concentrations more rapidly than predicted by the Hess model.[24,25] In the last two systems, the two polymers are slightly incompatible, but no upturn in D_f was reported.

In this contribution, we report the tracer diffusion of PS molecules in a porous medium filled with a PVME matrix solution in 2FT. As with the PS−PTHF−2FT system, we took advantage of the three-way index-matching between PTHF, 2FT, and silica. The compatibility of PS and PVME allowed us to increase the concentration of the matrix PVME; index-matching was still maintained at the highest concentrations studied. We limited the study here to the range of the matrix concentration from semidilute to concentrated,[26] because, below this range, the decay rate in the DLS autocorrelation functions for the diffusion process in the pore channels does not reach an asymptotic value even at long times and therefore it becomes difficult to estimate the long-time, macroscopic tracer diffusion coefficient in the porous medium. The same phenomenon was observed in the same concentration range for the PS−PTHF−2FT system. Below, we will show DLS results for tracer diffusion in the entangled matrix PVME in the porous medium. We were especially concerned to see if the slower decrease in D_p at high c_{mE}, observed for the PS−PTHF system with a low PS molecular weight, appears also in the PS−PVME system. We also discuss diffusion processes of entangled chains in the confining geometry.

On the basis of earlier results, we recently proposed a novel fractionation scheme, which we termed enhanced partitioning fractionation and which in principle could be aimed at processing-scale fractionation.[27,28] The scheme utilizes the segregation of polydisperse polymers that takes place between pore channels and the surrounding reservoir when the polymer solution in the reservoir is in the semidilute regime.[28] Concentration equilibrium is attained by migration of polymer chains through the maze of pore channels. Therefore, the equilibration times in this scheme are primarily determined by the self-diffusion coefficient of the polymer chain in the porous medium at high concentrations. The present studies provide an estimate of the required processing times.

Experimental Section

Dynamic Light-Scattering Measurement. The dynamic light-scattering (DLS) measurement system used in the present measurements has been described in detail elsewhere.[6,9,11] The light source was a 5 mW He−Ne laser, wavelength 632.8 nm. Two types of digital autocorrelator were used. A model N4SD (Coulter Electronics) with quasi-logarithmically spaced delay channels (the last channel is delayed by 3072 times the shortest delay time) was used for the DLS measurements of polymer solutions in the interior of a porous glass bead. For the measurements in the external free solution, we used either the N4SD or a Model 1096 (Langley-Ford Instruments, Coulter Electronics) equipped with 256 linearly spaced delay channels plus 16 additional delay channels for baseline detection. The scattering angles were 25.5 and 35.3°.

The normalized, baseline-subtracted intensity autocorrelation function $g_2(t)$ for scattering from external solutions was first converted to $g_1(t)$, where $g_1(t)$ is the magnitude of the normalized electric-field autocorrelation function, using $g_2(t) = [g_1(t)]^2$. Then $g_1(t)$ was analyzed by a second-order cumulant expansion: $\ln g_1(t) \cong -\langle\Gamma\rangle t + (\mu/2)t^2$. Here Γ is the decay rate in $g_1(t)$, $\langle\Gamma\rangle$ is its average, and μ is the variance of Γ. In contrast to the case of the external solution, the scattering from the interior of a glass bead directly provides $g_1(t)$. The autocorrelation function was then analyzed by the second-cumulant expansion and by a CONTIN[29] program that decomposes $g_1(t)$ into its spectrum $G(\Gamma)$ as $g_1(t) = \int e^{-\Gamma t}\Gamma G(\Gamma)\, d \ln \Gamma$.

Samples. Three different molecular weight fractions of polystyrene standards, PS050 ($M_p = 4.89 \times 10^4$; M_p is the peak molecular weight in size exclusion chromatography), PS100 ($M_p = 9.82 \times 10^4$), and PS170 ($M_p = 1.69 \times 10^5$) (Pressure Chemical), were used as probe polymers. The matrix polymer was poly(vinyl methyl ether) (PVME) (Aldrich). PVME has a broad molecular weight distribution. Size exclusion chromatography for PVME in tetrahydrofuran resulted in $M_p = 6.8 \times 10^4$ and $M_w/M_n = 2.7$ with reference to polystyrene standards, where M_w and M_n are the weight-average and number-average molecular weights, respectively.

In the experiments, a mixture of PS and PVME was dissolved in 2-fluorotoluene (2FT) (Aldrich). The mixture was known to be a single phase system at around room temperature for all compositions used. Spherical beads of controlled pore glass (Shell Development, S980G1.5) were used as the confining porous materials. The pore radius is about 250 Å, and the bead diameter is about 1.5 mm. The silica solid phase and the pore spaces constitute a bicontinuous structure. To avoid adsorption of polymers onto the pore walls, the surface was silanized with chlorotrimethylsilane as described elsewhere.[6] The solvent 2FT, the matrix polymer PVME, and silica, are nearly isorefractive at around 35 °C. Thus no significant decay components were observed in the DLS

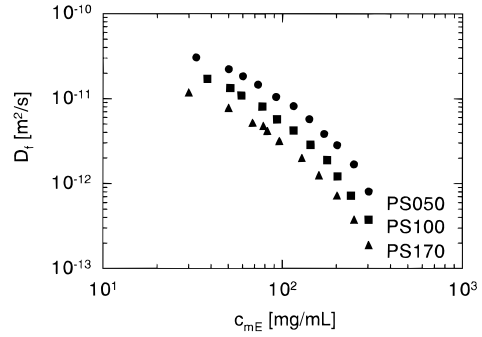

Figure 1. Tracer diffusion coefficients D_f of PS050, PS100, and PS170 in the exterior solution as a function of the external matrix concentration c_{mE}.

autocorrelation functions obtained from the interior of a porous glass bead immersed in a binary solution of PVME in 2FT over a wide range of concentrations, and PS was the only observable species in this three-way index-matched system both in the interior of a glass bead and in the exterior ternary solution.

The radii of gyration R_g of the probe polystyrene PS050, PS100, and PS170 are 81.2, 117, and 159 Å, respectively. These were calculated from the hydrodynamic radius R_H using $R_g/R_H = 1.562$.[30] These estimates are in good agreement with the reported values of R_g for polystyrene fractions in a good solvent.[31] The matrix PVME is expected to have $R_g \cong 97$ Å at the peak molecular weight M_p, if we assume that partitioning and retention times in the liquid chromatography are a function of R_g.

The concentration of the PS probe was held constant at one-fifth of the overlap concentration defined[30] by $(M_p/N_A)(\sqrt{2}R_g)^{-3}$, where N_A is Avogadro's number. The concentration of PVME ranged between 30 and 300 mg/mL. In terms of c_{mE}/c_m^* (where $c_m^* = 38.1$ mg/mL[32] is the overlap concentration of monodisperse PVME with a molecular weight equivalent to M_p of the polydisperse sample used), the concentration ranges from 0.79 to 7.9. Toward the higher end of the range, the matrix chains are considered to be entangled. At the highest concentrations ($\gtrsim$200 mg/mL), the solution is considered to have reached the concentrated regime.[26]

After complete dissolution of PVME and PS at the desired concentrations, the solution was poured into a test tube in which a porous glass bead was supported by a Teflon tube. The solution was filtered several times through a Millipore Teflon filter (0.2 μm). Equilibration times of at least 1 week were used before the DLS measurements from the interior of the bead began. All the measurements were performed at 34.8 °C. The refractive index of 2FT is ca. 1.460 at this temperature, and the viscosity of the solvent is 0.569 cP.[33]

Results

Diffusion in the Exterior Solution. The diffusivity of linear PS probes in a solution of PVME matrix in 2FT has been reported.[15−18] The main purpose of the present similar measurements of tracer diffusion in the exterior solution therefore was to provide a reference for the constrained diffusion of PS probe in the porous medium.

A plot of ln $g_2(t)$ against t showed a straight line followed by an upward deviation as ln $g_2(t)$ fell below −3 or −4. The average decay rate $\langle\Gamma\rangle$ in $g_1(t)$ and the breadth $\mu/\langle\Gamma\rangle^2$ were obtained by fitting $g_1(t)$ in the range of ln $g_1(t) \gtrsim -2$ to a second-order cumulant. As is often observed for nondilute polymer solutions, $\mu/\langle\Gamma\rangle^2$ was large, typically 4−7%, for all three PS samples over the entire range of c_{mE} measured. The diffusion coefficient D_f of the PS probe was calculated from the values of $\langle\Gamma\rangle$ at different scattering angles.

Figure 1 shows D_f as a function of c_{mE} for PS050, PS100, and PS170. The data are not corrected for a change in the monomer friction coefficient at high matrix concentrations. Values of D_f in the absence of the matrix polymer, D_{f0}, are 7.62×10^{-11}, 5.30×10^{-11}, and 3.81×10^{-11} m²/s, for these three samples.

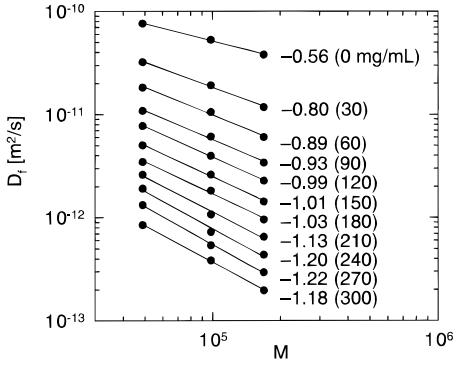

Figure 2. Tracer diffusion coefficients D_f at fixed matrix concentrations (given in parentheses), interpolated from the measured values, plotted against the molecular weight M of the polystyrene probe. The straight lines are the best fit to the power law $D_f \propto M^{\alpha_f}$. The exponents α_f are shown adjacent to the best fit lines.

The difference in D_f for different PS molecular weights increases as c_{mE} increases. To examine the dependence of D_f on the molecular weight M of the probe PS, we estimated D_f at given values of c_{mE} (indicated in parentheses in Figure 2), by interpolation of data measured at close values of c_{mE}, and plotted the estimated D_f against M, as shown. We then calculated the exponent α_f by curve-fitting the data to $D_f \propto M^{\alpha_f}$ at each matrix concentration. The values of α_f thus obtained are indicated adjacent to the fitted curve (Figure 2). In the absence of the matrix polymer, $\alpha_f = -0.56$. As c_{mE} increases, α_f decreases from −0.80 at $c_{mE} = 30$ mg/mL to −1.20 at $c_{mE} > 200$ mg/mL. These exponents are close to those obtained by Wheeler and Lodge[17,18] for PS probes that have a molecular weight higher than that of the matrix PVME in the respective concentration ranges. As noted, both constraint release and reptation mechanisms will contribute to the overall diffusion of probe chains in the entangled matrix chains, if the molecular weights of the probe polymer and the matrix polymer are not much different. If the probe polymer chains diffuse by a constraint release mechanism, the presence of the matrix polymer increases the effective solvent viscosity and, at the same time, shields the hydrodynamic interaction between segments on the probe chain. Then, the frictional force exerted on the probe chain is proportional to M, and α_f should be −1 (Rouse-like motion). When a reptation mechanism is also available, it will increase D_f. The increase will be more evident for a shorter probe chain, and therefore α_f will become smaller than −1 (crossover effect). For a sufficiently large M, α_f is expected to approach −1.

Diffusion in the Interior of the Porous Medium. The autocorrelation function $g_1(t)$ for the ternary polymer solution in the porous glass bead was measured at different c_{mE}. A substantial deviation from a single exponential decay was observed for $g_1(t)$ in the entire range of c_{mE} measured for all the PS samples. Unlike $g_2(t)$ for the exterior solution, the deviation was evident also at short time scales. These characteristics of $g_1(t)$ are similar to those observed in the PS/PTHF system reported earlier.[11] The spectrum $\Gamma G(\Gamma)$ of $g_1(t)$ obtained by CONTIN is shown for PS100 at the scattering angle of 25.5° for each c_{mE} in Figure 3. The main peaks are in general broader compared with the one observed in the absence of the matrix polymer.[11] Furthermore, CONTIN always separated out in the $G(\Gamma)$ spectrum an

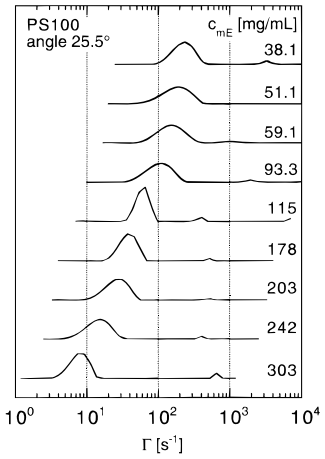

Figure 3. Spectrum $\Gamma G(\Gamma)$ of $g_1(t)$ obtained by CONTIN shown for PS100 at the scattering angle of 25.5° for each matrix concentration c_{mE}, indicated adjacent to each curve.

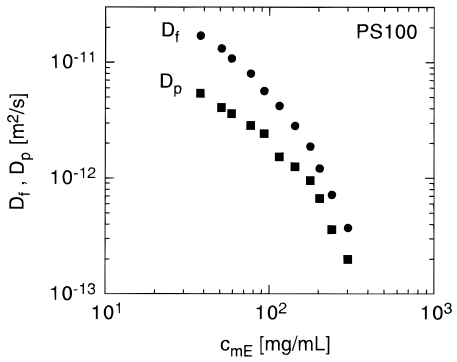

Figure 4. Tracer diffusion coefficients D_f and D_p of PS100 in PVME matrix solution within the porous glass bead and in the exterior solution, plotted as a function of the exterior matrix concentration c_{mE}.

additional peak at a frequency higher than the main peak. The time resolution of our measurement system was, however, not sufficient to evaluate the decay rate at short times. In our preceding contribution,[11] we speculated that a probe PS molecule can diffuse more rapidly in short sections of the pore channels without being blocked by matrix PTHF molecules, a process limited by the encounters of PS with matrix molecules.

To obtain the long-time decay rate in $g_1(t)$, the second-cumulant analysis was applied to the data in the range $-0.5 \gtrsim \ln g_1(t) \gtrsim -4$ in which $\ln g_1(t)$ followed a relatively linear behavior. The average decay rate $\langle\Gamma\rangle$ thus obtained agreed within a few percent with the average decay rate of the main peak in the spectrum obtained by CONTIN.

Below the concentration range discussed here, the deviation of $g_1(t)$ from a single exponential decay was greater. The $G(\Gamma)$ spectrum simply broadened and did not allow us to determine the macroscopic diffusion coefficient.

The diffusion coefficient D_p of probe polymer in the porous glass bead was calculated from the value of $\langle\Gamma\rangle$ at different scattering angles. To compare the diffusion coefficients D_f and D_p, we show them in Figure 4 as a function of the exterior matrix concentration c_{mE} for PS100. Note that c_{mI}, the PVME concentration in the pore channels, was not measured. The data are not corrected for any change in the monomer friction coefficient in the respective environment. The difference between D_f and D_p plotted on a logarithmic scale decreases as c_{mE} increases to 200 mg/mL. At $c_{mE} > 200$ mg/mL, D_f and D_p decrease in parallel. The tendency is similar for PS050 and PS170. We discuss this tendency in the following section.

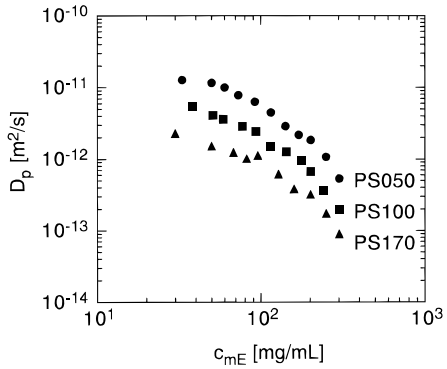

Figure 5. Tracer diffusion coefficients D_p of PS050, PS100, and PS170 in the porous glass bead plotted against the external matrix concentration c_{mE}.

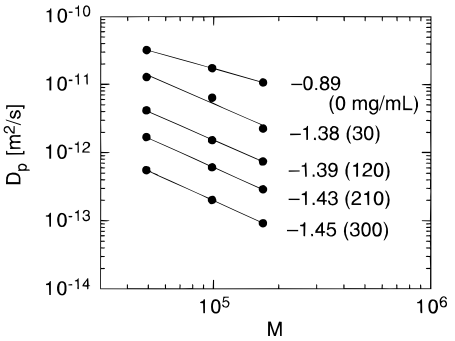

Figure 6. Tracer diffusion coefficients D_p at given matrix concentrations (given in parentheses), interpolated from the measured values, plotted against the molecular weight M of the probe polystyrene. Straight lines are the best fit to the power law $D_p \propto M^{\alpha_p}$. The exponents α_p are shown adjacent to the best fit lines.

Figure 5 shows the tracer diffusion coefficient D_p for PS050, PS100, and PS170. Values of D_p in the absence of matrix polymer, D_{p0}, are 3.13×10^{-11}, 1.96×10^{-11}, and 1.11×10^{-11} m^2/s, for the three samples. The tendency for a slower decrease in D_p and leveling-off, especially for PS050, observed in the less compatible PS−PTHF system, is not seen here. The diffusion coefficients decrease more rapidly at higher matrix concentrations. The difference in D_p among the three molecular weights of polystyrene is almost the same throughout the entire range of c_{mE} studied. In a similar fashion, we calculated D_p at selected values of c_{mE} (in parentheses, Figure 6) by interpolation of measured data. Figure 6 shows a plot of D_p as a function of probe molecular weight M. The data points are approximated by a power law $D_p \propto M^{\alpha_p}$. The forced curve-fit is shown together with the optimal value of α_p. The exponent α_p falls between −1.38 and −1.45 for 30 mg/mL < c_{mE} < 300 mg/mL. In the absence of PVME, $\alpha_p \cong -0.89$.

Discussion

Experimental studies of tracer diffusion of probe polymers in a solution of entangled matrix polymer have been primarily motivated by expectations that the studies might assist in the interpretation of the dynamics of entangled linear chains.[15−18] Reptation and constraint release modes have been critically examined on the basis of the results obtained. It appears relevant to examine in this perspective our results that compare probe polymer diffusion in entangled matrix chains in

free space and in a restricted geometry. We will consider how the center of mass tracer diffusion coefficient D_p in high matrix concentrations in the pore should change from the diffusion coefficient D_f in the external solution, when compared at the same matrix concentration.

We note that the high matrix concentrations change the monomer friction coefficient ζ considerably from its value ζ_0 in the dilute solution limit. As an experimentally verified formula,[18] we employ

$$\zeta/\zeta_0 = (1 + \phi_m)^2/(1 - \phi_m)$$

where ϕ_m is the volume fraction of the matrix polymer in the solution. Since ϕ_m is in general different between the interior of the porous medium and the exterior to the pore, the two diffusion coefficients D_p and D_f need to be adjusted for the monomer friction coefficients ζ_p and ζ_f, respectively. We therefore compare $D_p\zeta_p/\zeta_0$ and $D_f\zeta_f/\zeta_0$.

In the reptation hypothesis,[1,2] the macroscopic center of mass diffusion is made possible by one of the chain ends freely choosing the direction of the next step motion as all the other segments follow the primitive path in the fixed matrix. The degree of freedom available to the chain ends does not depend on the chain length. When confined in a porous medium, certain paths are excluded from those available to the chain ends. The decrease in the degrees of freedom available to these ends, again, does not depend on the chain length. Therefore, the ratio of $D_p\zeta_p/\zeta_0$ to $D_f\zeta_f/\zeta_0$ is independent of the length of the probe chain and is equal to the ratio of D_p to D_f of a point mass in the absence of matrix chains:

$$D_p\zeta_p/D_f\zeta_f = \lim_{R_g \to 0} D_{p0}/D_{f0}$$

The ratio in the vanishing limit of R_g is smaller than unity because of pore tortuosity, and is a function of pore structure.[6]

We also consider the probe chain diffusion in terms of a constraint release mechanism. The difference in the elementary process between diffusion in the pore and that in the external solution is a longer step time for the former because of slower diffusion of confined matrix chains. In addition, the pore tortuosity reduces the rate of macroscopic motion of the probe chain in the porous medium. The second factor is held constant in a wide range of matrix concentrations from dilute to semidilute. Thus we can write

$$D_p\zeta_p/D_f\zeta_f = (D_{mp}\zeta_p/D_{mf}\zeta_f)(D_{p0}/D_{f0})$$

where D_{mf} and D_{mp} are the self-diffusion coefficients of entangled matrix chains in the exterior solution and in the pore, respectively. They are subject to the corrections to the monomer friction coefficients in the same way as D_f and D_p are. To release the constraint on the probe chain, the matrix chain has to move on a scale comparable to its own dimension. Therefore D_{mf} and D_{mp} are not the macroscopic diffusion coefficients but refer to the diffusion over a distance of the order of a matrix chain dimension. The pore tortuosity forces $D_{mp}\zeta_p/D_{mf}\zeta_f$ to depend on the chain dimension.[5,6] When the matrix chain is smaller than the pore size, $D_{mp}\zeta_p/D_{mf}\zeta_f = 1$ and decreases as the matrix chain increases in size. The second factor D_{p0}/D_{f0} is a decreasing function of the molecular weight of the probe polymer.[6,8]

Thus the dependence of $D_p\zeta_p/D_f\zeta_f$ on the molecular weight M of the probe chain and the matrix concentration c_m in the reptation and constraint release mechanisms is $D_p\zeta_p/D_f\zeta_f \sim M^0{c_m}^0$ and $D_p\zeta_p/D_f\zeta_f \sim (D_{p0}/D_{f0})M^0{c_m}^0$, respectively. Here we took into account that the matrix PVME chains used are smaller than the pore size. In the second expression, $D_p\zeta_p/D_f\zeta_f$ depends on M as does D_{p0}/D_{f0}. In the DLS experiments for $c_{mE} > 200$ mg/mL, we found that $D_p/D_f \sim M^{\alpha_p - \alpha_f}$, where $\alpha_p - \alpha_f \cong -0.24 \pm 0.03$, and $D_{p0}/D_{f0} \sim M^{-0.33}$. The matching of the exponents therefore favors the constraint release mechanism. Note that M dependence is not subject to the change in ζ.

To estimate ζ_p/ζ_0 and to compare $D_p\zeta_p/\zeta_0$ and $D_f\zeta_f/\zeta_0$ at the same matrix concentration in a wide range, it is necessary to calculate the interior matrix concentration c_{mI} for a given external concentration c_{mE}. However in our measurements the matrix polymer is polydisperse and the high osmotic pressure of the semidilute external solution will drive PVME into pore channels, but the forced migration favors low molecular weight components.[27] Because the molecular weight distribution will be different between the interior of the pore and the exterior, comparison between $D_p\zeta_p/\zeta_0$ and $D_f\zeta_f/\zeta_0$ at the same weight concentration is less meaningful. We therefore employ a reduced concentration X defined, for a polydisperse polymer solution, as[34]

$$X = \sum_j \frac{X_j}{(M_j/M_n)^{3\nu}}$$

where $\nu \cong 0.588$ and X_j is the partial reduced concentration of fraction j with molecular weight M_j, which is defined as[9,30]

$$X_j = 3.49 c_j/c_j^*$$

for partial concentration c_j. The overlap concentration c_j^* refers to that of the solution of fraction j alone. Scaling theory predicts[1] that an osmotic pressure of a semidilute polymer solution reduced by its ideal solution functional form c_jRT/M, where R is the gas constant and T the temperature, is a function of c_j/c_j^*. The same rule applies to the diffusion coefficient. Thus we can compare $D_p\zeta_p/\zeta_0$ and $D_f\zeta_f/\zeta_0$ at the same reduced concentration.

For simplicity, we assume that the molecular weight distribution of PVME follows a log-normal distribution, and that the pore channels are composed of straight cylinders throughout the medium. The total reduced concentration X is related to $\bar{X}$, the reduced concentration for monodisperse PVME with molecular weight equal to M_p, by $X/\bar{X} = (M_w/M_n)^{(1-3\nu)/2} = 0.684$, compared at the same total weight concentration. We also used an estimate for R_g of PVME (at $M_p = 6.8 \times 10^4$) divided by the pore radius at 0.39.[32]

To solve the concentration equilibrium problem of the polydisperse system, we equilibrated the chemical potential of a polymer chain in the pore channels to that in the external solution for all fractions. The reduced interior concentration X_{mI} was computed at different reduced exterior concentrations X_{mE} of the matrix polymer in the range of $X_{mE} < 40$. The partition coefficient p_{Xm} defined as the ratio of X_{mI} to X_{mE} is plotted in Figure 7. The range studied here for DLS measurements is $1.88 < X_{mE} < 18.8$. The curve can be well approximated by $p_{Xm} \cong a_1 + a_2 \tanh[a_3(\ln X_{mE} - a_4)]$ with $a_1 = 0.600\,41$, $a_2 = 0.391\,30$, $a_3 = 0.751\,20$,

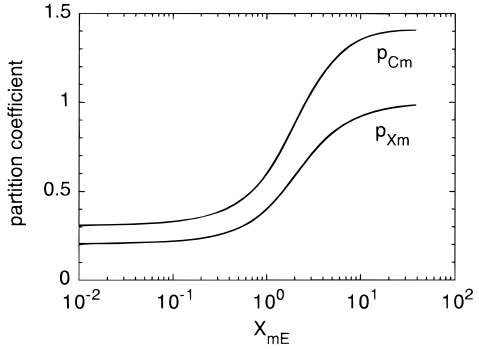

Figure 7. Partition coefficients p_{Xm} and p_{Cm} of polydisperse PVME calculated as a function of the reduced exterior concentration X_{mE}. See text for definitions.

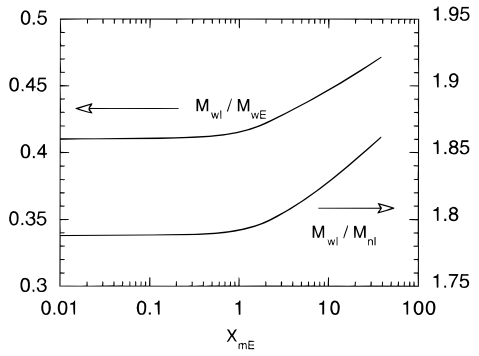

Figure 8. Ratio of the weight-average molecular weight of the matrix polymer in the porous medium to that in the exterior solution, M_{wI}/M_{wE}, and the ratio of the weight-average molecular weight to the number-average molecular weight of the matrix polymer in the pore, M_{wI}/M_{nI}, plotted as a function of X_{mE}.

and $a_4 = 0.740\,76$. Also shown in the figure is the partition coefficient p_{Cm} defined as $p_{Cm} \equiv c_{mI}/c_{mE}$. Because of the partitioning inversion for low molecular weight components,[27] the overall concentration of PVME becomes higher in the pore than in the exterior solution at $X_{mE} > 2.7$. The second curve can be approximated by the equation given above with $a_1 = 0.871\,15$, $a_2 = 0.554\,54$, $a_3 = 0.788\,44$, and $a_4 = 0.666\,17$.

We also calculated M_{wI}/M_{wE}, the ratio of the weight-average molecular weight of the matrix polymer in the porous medium to that in the exterior solution, and M_{wI}/M_{nI}, the ratio of the weight-average molecular weight to the number-average molecular weight of the matrix polymer in the pore, shown in Figure 8. At low X_{mE}, the interior solution is dominated by low molecular weight components. As X_{mE} increases, high molecular weight components are also driven into the pore channels by the high osmotic pressure of the exterior solution. In the range of X_{mE} relevant to the current DLS measurements, M_{wI}/M_{wE} ranges between 0.42 and 0.46.

Using the estimate of p_{Cm} and the formula for ζ/ζ_0, the tracer diffusion coefficients were corrected for the change in ζ in the porous medium and in the exterior solution. In Figure 9, $D_f\zeta_f/\zeta_0$ and $D_p\zeta_p/\zeta_0$ are plotted against X_m (X_{mE} and X_{mI}, respectively), for PS100. Apparently, corrections due to the change in the monomer friction do not have a significant effect on the difference between the two diffusion coefficients. The same trend was observed for PS050 and PS170.

Considering $D_p\zeta_p/D_f\zeta_f$, we calculated, by interpolation of measured data, $D_f\zeta_f/\zeta_0$ at an X_{mE} equal to X_{mI} at which D_p was measured. Figure 10 shows $D_p\zeta_p/D_f\zeta_f$ obtained

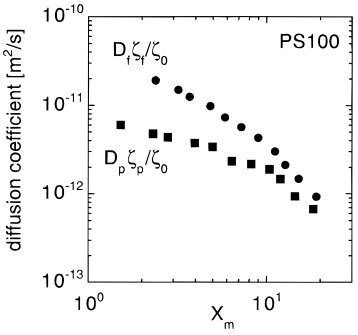

Figure 9. Tracer diffusion coefficients $D_f\zeta_f/\zeta_0$ and $D_p\zeta_p/\zeta_0$, corrected for the change in the monomer friction coefficients, of PS100 in the PVME matrix solution plotted as a function of the reduced matrix concentration X_m.

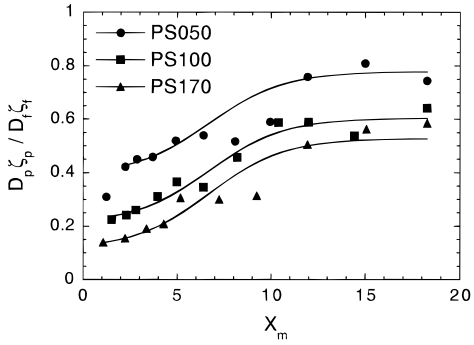

Figure 10. Ratio of the tracer diffusion coefficient in the porous medium to that in the external solution, $D_p\zeta_p/D_f\zeta_f$, plotted as a function of reduced matrix concentration X_m. Lines shown for convenience.

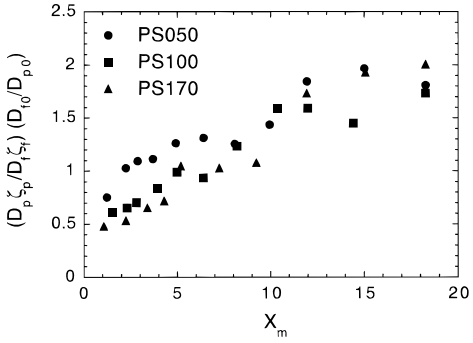

Figure 11. Product of $D_p\zeta_p/D_f\zeta_f$ and its reciprocal in the dilute matrix concentration limit plotted as a function of the reduced matrix concentration X_m.

in this way for PS050, PS100, and PS170. If the probe chain moves by reptation, the data points should collapse onto a master curve of $D_p\zeta_p/D_f\zeta_f = \lim_{R_g\to 0}(D_{p0}/D_{f0}) \cong 0.9$. The value in the vanishing limit of R_g was obtained from the previous measurements.[8] A difference exists between the three polystyrene samples at high matrix concentrations. Thus we conclude again that probe chains do not appear to diffuse with a reptation mechanism.

To see if the constraint release mechanism is applicable, we plot in Figure 11 $(D_p\zeta_p/D_f\zeta_f)(D_{f0}/D_{p0})$. The agreement between data points for different molecular weights of the probe polymer is much better than that in Figure 10. The absolute value of $(D_p\zeta_p/D_f\zeta_f)(D_{f0}/D_{p0}) = D_{mp}\zeta_p/D_{mf}\zeta_f$, which should be equal to or smaller than unity for a monodisperse matrix polymer, is larger than unity. The step time for the constraint release is shorter in the pore than in the exterior solution. This apparent contradiction is probably based on the difference in the

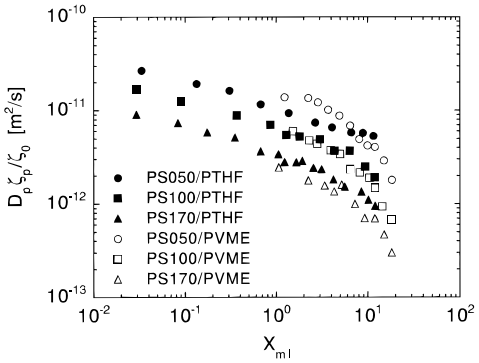

Figure 12. Tracer diffusion coefficients of PS probes of three different molecular weights in the porous medium in ternary solutions of PTHF matrices (closed symbols) and of PVME matrices (open symbols), plotted as a function of the reduced matrix concentration X_{mI} in the porous medium.

molecular weight distribution. As seen in Figure 8, the average chain length of the matrix polymer in the pore is about half of that in the exterior solution. If the matrix polymer diffuses by a Rouse-like mechanism at high matrix concentrations, $D_{mp}\zeta_p/D_{mf}\zeta_f$ will be around 2.

Finally, we compare two tracer diffusion coefficients of probe PS, one measured in a PTHF solution reported earlier,[11] and the other measured in a PVME solution. For this purpose, we calculated the partition coefficient of the monodisperse PTHF with $R_g/R_p = 0.676$. The change in the monomer friction coefficient was taken into account, but the correction in D_p was negligible, because $c_{mI} < 40$ mg/mL. Figure 12 shows the two tracer diffusion coefficients plotted as a function of X_{mI}, the reduced concentration of the matrix polymer (PTHF or PVME) in the porous medium. Except for PS050 that may have been affected by incipient phase separation, overlap between the two sets of data is good. We can conclude, therefore, that the macroscopic diffusion coefficient over a long time in the porous medium is insensitive to the nature of the polymer-polymer interaction, as long as the solution system is in a single phase. Reduction in D_p is primarily caused by the matrix chains hindering the probe chains from moving past the matrix chains in the narrow pore channels.

Conclusions

Dynamic light-scattering measurements for the tracer diffusion of probe polystyrene in a semidilute solution of compatible poly(vinyl methyl ether) in a porous medium have shown a complex behavior. The leveling-off of the tracer diffusion coefficient, observed for polystyrene in the pore as the concentration of matrix poly(tetrahydrofuran) increased, was not repeated in the present highly compatible system. We can therefore conclude that the leveling-off reflects macromolecular repulsion. Because the leveling-off was not observed for the tracer diffusion in the exterior solution at the same matrix concentrations, we may conclude that the effect of chain−chain interaction is enhanced by narrow pores.

Both reptation and constraint release mechanisms were considered in the analysis of the diffusion of the probe polymer in a semidilute solution of matrix polymer in a porous medium. It is possible, by comparing the diffusion coefficient in the porous medium and that in the exterior solution, to determine which of the two mechanisms dominates in the diffusion process. For the samples used in the present contribution, we find the data quite strongly support the constraint release mechanism, although the matrix polymer used was polydisperse. In future work it seems essential to repeat the tracer diffusion measurement using a monodisperse matrix polymer; the dependence on the molecular weight of the matrix polymer also needs to be explored.

Acknowledgment. This contribution was supported in part by the Air Force Office of Scientific Research through the grant No. AFOSR 94−001.

References and Notes

(1) de Gennes, P. G. *Scaling Concepts in Polymer Physics*; Cornell University Press: Ithaca, NY, 1979.
(2) Doi, M.; Edwards, S. F. *The Theory of Polymer Dynamics*; Clarendon Press: Oxford, U.K., 1986.
(3) Kärger, J.; Lenzner, J.; Pfeifer, H.; Schwabe, H.; Heyer, W.; Janowski, F.; Wolf, F.; Zdanov, S. P. *J. Am. Ceram. Soc.* **1983**, *66*, 69.
(4) Dozier, W. D.; Drake, J. M.; Klafter, J. *Phys. Rev. Lett.* **1986**, *56*, 197.
(5) Bishop, M. T.; Langley, K. H.; Karasz, F. E. *Phys. Rev. Lett.* **1986**, *57*, 1741.
(6) Bishop, M. T.; Langley, K. H.; Karasz, F. E. *Macromolecules* **1989**, *22*, 1220.
(7) Easwar, N.; Langley, K. H.; Karasz, F. E. *Macromolecules* **1990**, *23*, 738.
(8) Guo, Y.; Langley, K. H.; Karasz, F. E. *Macromolecules* **1990**, *23*, 2022.
(9) Teraoka, I.; Langley, K. H.; Karasz, F. E. *Macromolecules* **1993**, *26*, 287.
(10) Daoud, M.; de Gennes, P. G. *J. Phys. (Paris)* **1977**, *38*, 85.
(11) Zhou, Z.; Teraoka, I.; Langley, K. H.; Karasz, F. E. *Macromolecules* **1994**, *27*, 1759.
(12) Brown, W.; Pu, Z. *Macromolecules* **1990**, *23*, 5097.
(13) Brown, W.; Pu, Z. *Macromolecules* **1991**, *24*, 1820.
(14) Brown, W.; Nicolai, T. In *Dynamic Light Scattering*; Brown, W., Ed.; Clarendon Press: Oxford, U.K., 1993.
(15) Lodge, T. P. *Macromolecules* **1983**, *16*, 1393.
(16) Lodge, T. P.; Wheeler, L. M. *Macromolecules* **1986**, *19*, 2983.
(17) Wheeler, L. M.; Lodge, T. P.; Hanley, B.; Tirrell, M. *Macromolecules* **1987**, *20*, 1120.
(18) Wheeler, L. M.; Lodge, T. P. *Macromolecules* **1989**, *22*, 3399.
(19) Nyström, B.; Roots, J. *Macromolecules* **1991**, *24*, 184.
(20) Brown, W.; Pu, Z. *Macromolecules* **1989**, *22*, 3508.
(21) Brown, W.; Pu, Z. *Macromolecules* **1989**, *22*, 4031.
(22) Numasawa, N.; Kuwamoto, K.; Nose, T. *Macromolecules* **1986**, *19*, 2593.
(23) Nemoto, N.; Inoue, T.; Makita, Y.; Tsunashima, Y.; Kurata, M. *Macromolecules* **1985**, *18*, 2516.
(24) Hess, W. *Macromolecules* **1986**, *19*, 1395.
(25) Hess, W. *Macromolecules* **1987**, *20*, 2587.
(26) Graessley, W. W. *Polymer* **1980**, *21*, 258.
(27) Teraoka, I.; Zhou, Z.; Langley, K. H.; Karasz, F. E. *Macromolecules* **1993**, *26*, 3223.
(28) Teraoka, I.; Zhou, Z.; Langley, K. H.; Karasz, F. E. *Macromolecules* **1993**, *26*, 6081.
(29) Provencher, S. W. *Macromol. Chem.* **1979**, *180*, 201.
(30) des Cloizeaux, J.; Jannink, G. *Polymers in Solution: Their Modelling and Structure*; Clarendon Press: Oxford, U.K., 1990.
(31) Huber, K.; Bantle, S.; Lutz, P.; Burchard, W. *Macromolecules* **1985**, *18*, 1461.
(32) Calculated on the basis of the data in ref 18.
(33) Viswanath, D. S.; Natarajan, G. *Data Book on the Viscosity of Liquids*; Hemisphere: New York, 1989.
(34) Ohta, T.; Oono, Y. *Phys. Lett.* **1982**, *89A*, 460.

MA950016N